Astron. Astrophys. 319, 561–577 (1997)

ASTRONOMY
AND
ASTROPHYSICS

Chemical composition of optically bright post-AGB stars⋆

Hans van Winckel

Instituut voor Sterrenkunde, K.U.Leuven, Celestijnenlaan 200B, B-3001 Heverlee, Belgium

Received 9 April 1996 / Accepted 19 August 1996

Abstract. We present a detailed LTE chemical analysis of 10 optically bright F-type post-AGB objects on the basis of the analysis of high-resolution optical spectra and compare the results with similar objects discussed in the literature.

The iron content is low on average, and so confirms the old and hence low-mass nature of the supergiants, with a noticable exception of HD 95767.

We emphasize the fact that the chemical patterns observed are very diverse : several different classes can be distinguished. Only a minor fraction of the objects are conform to standard post third dregde-up theory. Only in HD 187885 (Van Winckel et al., 1996), HD 56126 (Klochkova, 1995) and HD 158616 (this paper) is there conclusive *chemical* evidence that they occur in a post-AGB evolutionary phase : a high total CNO abundance, for HD 187885 a supersolar He content and–above all–a large overabundance of s-process elements.

The other objects, together with other well studied high galactic latitude F-supergiants, display no s-process enhancement but even depletion in some cases. The high N abondance and the mildly enhanced total CNO abundance indicate that the atmospheres of these objects contain a mixture of CNO-cycled material and He-burning products. For some sources, however, this enhancement of the total CNO abundance is barely significant.

HD 107369, the only object in our sample with neither Hα emission nor observed IR excess, displays also unique chemical patterns among our sample stars (a C deficiency coupled with a moderate Fe depletion of [Fe/H] = $-$ 1.1). This star is the only object in our sample showing similar chemical patterns to the metal poor B stars at high galactic latitude (Conlon et al., 1993). Our chemical analysis does therefore not point to an evolutionary connection between the dusty high-latitude supergiants and the metal-poor B stars, but rather suggests that the latter evolve from stars such as HD 107369.

Key words: stars: abundances – stars: evolution – stars: individual: SAO 173329, HD 95767, SAO 239853, HD 107369, HD 108015, HD 112374, HD 131356, HD 133656, HD 158616, HD 187885 – stars: AGB and post-AGB

Send offprint requests to: Hans Van Winckel
(hans@ster.kuleuven.ac.be)

⋆ Based on observations obtainted at ESO, and the Swiss telescope at La Silla

1. Introduction

Although some post-AGB stars were known before the launch of IRAS (e.g. AFGL 618, AFGL 2688 = the "Egg Nebula"), our knowledge of the late stages of stellar evolution is greatly determined by the infrared survey of this satellite. The IRAS ((12)-(25)) - ((25)-(60)) colour-colour diagram has been successfully used by several authors in systematic searches for post-AGB objects by looking for sources in-between the locus of the planetary nebulae and late-type AGB stars (Kwok, 1986; Kwok et al., 1987; van der Veen et al., 1989; Volk and Kwok. 1989; Manchado et al., 1989; Slijkhuis, 1992). The selection criteria of these authors implicitly assume that the positions of the transition objects in the IRAS colour-colour diagram are only determined by the expanding dust-shell. Most objects selected this way still suffer from large amounts of circumstellar extinction and do not have optical counterparts or only very faint ones.

Another approach to look for transition objects was concentrated on optically bright objects with an IR excess due to circumstellar dust (Hrivnak et al., 1989; Pottasch and Parthasarathy, 1988; Waelkens et al., 1989; Trams et al., 1991; Oudmaijer et al., 1992). These resulted in the detection of objects scattered in the IRAS colour-colour diagram, as they show different amounts of IR excesses and different IR-colours. Interestingly most high-latitude supergiants were recovered in these studies, strengthening the idea that the F-G supergiants at large distance from the galactic plain as discovered by Bidelman (1951), are not population I objects, but low-mass stars in the late stages of stellar evolution. The high latitude, on average low metal content, and in some cases high space motion are observational indications for the old and hence low-mass population of these objects. Current evolutionary tracks through the location of the F-type supergiants in the HR-diagram indicate them to be in a post-AGB evolutionary stage. As the objects resulting from the systematic searches are mostly supergiants

located at intermediate or high galactic latitude, they are also referred to as high galactic latitude supergiants.

Surface abundance determinations of these optically bright objects offer a powerful tool, not only to clarify the evolutionary nature of the objects themselves, but also to constrain chemical evolutionary calculations. For AGB-stars such studies are often difficult due to the cool temperature of the objects and the complex atmospherical structure. The optically bright F-G supergiants are ideally suited as tracers of the chemical evolution of low-mass stars as their effective temperature (typically between 7500-6500 K) and optical brightness allow accurate determination of the photospheric chemical content using standard LTE model-atmospheres.

Recent studies, however, show that rather complex and very diverse chemical patterns are observed and different chemical classes can be distinguished. There is a clearly separate group of extremely iron deficient stars, with iron abundances as low as [Fe/H] = -4.8, in which the photospherical chemical content is determined by gas accreted from the circumstellar dusty envelope (Venn and Lambert, 1990; Bond, 1991; Van Winckel et al., 1992, Mathis and Lamers, 1992, Waters et al., 1992). The abundance patterns observed in these stars resemble the depletion patterns of the gas phase of the interstellar medium. It is clear that the photospheric chemical content of these objects does not reflect the chemical changes brought by dredge-ups during the stellar evolution. As all objects turned out to be binaries with orbital periods in a rather limited range (Van Winckel et al., 1995), they represent a peculiar stage in binary evolution. Recently some other evolved stars have been detected that dispay the same chemical patterns: the binary ST Pup (Gonzalez and Wallerstein, 1996) and the RV Tauri variables IW Car, DY Ori, EP Lyr, AR Pup and RSge (Giridhar et al., 1994; and Gonzalez et al., 1996).

But also the more moderately deficient objects, whose chemical composition is thought to be the initial composition changed by the succesive dredge-ups, are far from chemically homogeneous. It is remarkable to note that in only a few hitherto studied objects, clear *chemical* evidence for a post-AGB phase of evolution is detected: only in HD 56126 (Klochkova, 1995) and in HD 187885 (Van Winckel et al., 1995) s-process elemental enhancements are detected together with high C/O ratios, as expected after dredge-up of material exposed to He-burning (3rd dredge-up). For most objects, the chemical patterns are more difficult to interpret.

In this paper, we will discuss the chemical composition of a selection of optically bright objects in a homogeneous way in order to study the wide chemical diversity within the post-AGB objects in more detail and to get better insight in the final stages of stellar chemical evolution of intermediate to low-mass stars.

In Sect. 2 we introduce our sample of programme stars, followed by a description of the observational programme (Sect. 3). In Sect. 4 we discuss our computational method and devote special attention to the determination of the model atmospherical parameters (T_{eff}, log(g), micro-turbulent velocity) and error analysis (Sect. 5). In Sect. 6 we cover the results for the individual objects in order to conclude with a more general discussion on the different chemical patterns observed and the implication on the chemical evolution of low-mass stars.

2. Programme stars

The programme stars given in Table 1 are a selection from the list of Oudmaijer et al. (1992) of good candidate low-mass post-AGB stars in the southern hemisphere with high or intermediate galactic latitude. These authors performed a cross-correlation of the SAO optical catalogue with the IRAS point-source catalogue, selecting supergiants with a spectral type between B and G with an IR excess due to circumstellar dust. Two more stars are included, HD 107369 for which no IR excess is measured and HD 133656 for which the 12 μm flux has a bad quality and thus does not fulfill the initial selection criteria, but for which an IR excess occurs at longer wavelengths (Oudmaijer, 1996).

Detailed studies of the spectral energy distribution (SED) of opticaly bright post-AGB candidate stars have shown that the objects can be devided into two groups, depending on the shape of the IR excess (Trams et al., 1991, van der Veen et al., 1994, Bogaert, 1994): sources with a broad IR excess extending from the near-IR until the far-IR have both hot and cool dust in their circumstellar shells and sources with only a far-IR excess show only the presence of cool dust. For our programme stars, the shape of the energy distibution is also given in Table 1. This classification is independent of the adopted photospheric parameters (T_{eff}, log(g), Z).

The radial velocities with respect to the local standard of rest are given in the last column of Table 1. These are the mean of the radial velocity measurements deduced from the different spectra (see later) and measurements obtained with the radial velocity meter CORAVEL mounted on the Swiss telescope at the Haute-Provence observatory.

2.1. Individual objects

2.1.1. SAO 173329

This star is a poorly studied post-AGB candidate. It displays optical variability (Bogaert, 1994) with a total amplitude of 0.055 magnitudes. The photometric data are too scarce to determine a period. Interestingly, SAO 173329 is the only object in our sample that displays a strong P-Cygni Hα line profile (Waters et al., 1993) with an outflow velocity of not less then 300 km/s, which is highly remarkable for an F-type supergiant.

2.1.2. HD 95767

This visual binary was also classified by other authors as a candidate post-AGB star (Volk and Kwok, 1987; Pottasch and Parthasarathy, 1988) on the basis of the IR excess and the low resolution IRAS spectrum.

It probably is a pulsating star with a quasi period of 103 days and a total amplitude of 0.144 magnitudes (Bogaert, 1994). The star is located in the Cepheid instability strip, but the period is rather long for a classical Cepheid. It is the only object in our sample that is located in the galactic plane.

Table 1. The programme stars.

Nr.	Star	α_{2000} h m s	δ_{2000} ° ′ ″	b °	m_v	Hot DUST	Cool DUST	V_{LSR} km/s
1	SAO 173329	07 16 08	−23 27 01	−5°	10.6	Y	Y	+58
2	HD 95767	11 02 04	−62 09 42	−2°	8.8	Y	Y	−36
3	SAO 239853	12 20 15	−53 55 31	+9°	9.3	N	Y	+33
4	HD 107369	12 20 45	−32 33 26	+30°	9.6	N	N	−42
5	HD 108015	12 24 53	−47 09 07	+15°	7.9	Y	Y	−2
6	HD 112374	12 56 30	−26 27 35	+36°	6.6	N	Y	−26
7	HD 131356	14 57 00	−68 50 22	−9°	8.7	Y	Y	−14
8	HD 133656	15 07 27	−48 17 53	+8°	7.5	N	Y	−10
9	HD 158616	17 30 47	−11 22 08	+12°	9.6	Y	Y	+71
10	HD 187885	19 52 52	−17 01 49	−21°	8.6	N	Y	+25

2.1.3. SAO 239853

SAO 239853 was first classified as a post-AGB candidate star by Hrivnak et al. (1989) on the basis of the IRAS colours. The energy distribution is discussed by Bogaert (1994) who also found the star to be a pulsating variable with a period of 37 days and a total amplitude of 0.103 magnitudes in V.

2.1.4. HD 107369

This star, first classified as a horizontal branch (HB) star, was found to have a much larger Strömgren photometric index c_1 than usual for HB stars, pointing to a low gravity (Philip, 1972). Bond and Philip (1973) pointed out the photometric similarity between the star and the extremely metal deficient high galactic object BD+39°4926.

Kodaira and Philip (1984) performed a chemical analysis of the star based on high dispersion photographic spectra and concluded that the star may have an almost normal iron abundance but a large radial velocity ($V_r = -45 \pm 3$ km s^{-1}) for a Population I star and thus concluded that the star is in a stage where it evolves from the blue horizontal branch.

The star is probably different from the other stars in the sample : it was not detected by IRAS and it does not show any Hα emission, two characteristics present in all the other sources. We include the star nevertheless because it is at a high galactic latitude and it appeared metal deficient in our low resolution spectra.

2.1.5. HD 108015

This object was also classified as a post-AGB candidate by other authors (Volk and Kwok, 1987; Pottasch and Parthasarathy, 1988) who discussed the IR excess due to circumstellar dust. Eggen (1991) listed the star as being highly luminous or composite.

Our photometric observations prove it to be a variable star with a total amplitude of 0.135 magnitudes, but with variable lightcurves in the different observing seasons (Bogaert, 1994).

2.1.6. HD 112374

HD 112374 (HR 4912; LN Hya) is a semi-regular variable with a period of 44, 53 or 69 days and an amplitude of 0.3 magnitudes in V (Eggen 1986 and references therein). The mean radial velocity is found to be -22 km s^{-1}. The colour variations of the Geneva photometry obtained at La Silla are anomalous and the slope in the (U-B)-m$_v$ diagram points to variable circumstellar extinction (Bogaert, 1994). The shape and amplitude of the lightcurve differ from one observing season to another. The circumstellar dust is relatively cool and thus already far from the star indicating that the shell was formed long ago, probably during the AGB evolution (Trams et al., 1991).

The chemical composition was discussed by Luck et al. (1983). We did not obtain enough data on this star to perform a complete independent analysis and therefore we will adopt the results from these authors in the general discussion.

2.1.7. HD 131356

HD 131356 (EN TrA) was first classified as a normal Cepheid variable but from the alternating deep and shallow minima and phase lag between the light and colour curves, Pel (1976) classified it as a RV Tauri star. The period is found to be between 34 and 37 days as given by Grayzeck (1978) and Evans (1985) with a total amplitude of about 0.8 magnitudes in V. The photometry obtained by the Geneva Telescope is too scarce to determine a period accurately (Bogaert, 1994). The position and mean heliocentric radial velocity are found to be anomalous for normal population I stars (Grayzeck, 1978). The same author could not find evidence for Hα line emission. Evans (1985) classified EN TrA as a RVa type, noting no variations in the mean magnitude. It is the only known RV Tauri star in our sample.

2.1.8. HD 133656

HD 133656 was remarked on by Oudmaijer (1996) during a search for stars in the IRAS point source catalogue for objects that were not listed at 12 μm with a well determined flux density but had an excess at 25 and 60 μm . On the low resolution spectra obtained by Oudmaijer the star appeared metal deficient.

Our Geneva photometry obtained until now (14 measurements) did not show any variability, neither on a long timescale (15 years), nor during short time-intervals (2 times 2 measurements in respectively 40 and 6 days).

We included this intermediate galactic latitude object in our programme as it appeared metal deficient on the low resolution spectra obtained by Oudmaijer.

2.1.9. HD 158616

In the photometric programme this star turned out to be a pulsating variable with some RV-Tauri like characteristics. Bogaert (1994) identified 2 possible periods (P_1 = 93 and P_2 = 61 days) but more photometric data are definitely needed to confirm these findings. This star was not yet discussed by other authors.

2.1.10. HD 187885

HD 187885 is a high galactic latitude F-supergiant which shows a strong far-IR excess as found also by Parthasarathy and Pottasch (1986) and Hrivnak et al. (1989). In a later paper Parthasarathy et al. (1988) discuss IUE observations and conclude that, although their low resolution optical spectrum is consonant with a spectral classification of a F2-3 I supergiant, the UV flux indicates a much hotter source. HD 187885 is one of the rare sources in our sample that is detected in the ^{12}CO and ^{13}CO J=1-0 and J=2-1 lines (Likkel et al., 1987; Bujarrabal et al., 1992).

From the CO detection an expansion velocity of 13 km s^{-1} is deduced (van der Veen et al., 1993). The circumstellar material is found to be probably carbon rich as indicated by the strength of the HCN line compared to CO lines and from the possible detection of the 11 μm feature in the IRAS LRS spectrum together with the absence of OH and H_2O maser emission (Bujarrabal et al., 1992). In the ^{12}CO line profile there is evidence for two components with the main component having an expansion velocity of 13 km s^{-1}, and a higher velocity component with an outflow velocity of 40 km s^{-1}.

3. Observational programme

The chemical analysis of the programme stars is based on high resolution ($\lambda/\delta\lambda$ = 50 000 − 55 000 corresponding to a projected slit width between 2.5" and 2.0"), high signal-to-noise (S/N > 70), spectra obtained with the Coudé Echelle Spectrometer (CES) fed by the 1.4m Coudé Auxiliary Telescope (CAT) at ESO La Silla. This echelle spectrograph is not equipped with a cross-disperser and therefore measures only one order at the time, this order being selected by a pre-disperser. The log of the observations for each star can be obtained from the author upon request. Most spectra were measured during several runs specially devoted to this programme; they were supplemented with spectra obtained during the Hα monitoring programme of the same stars and during test and reserved time of the La Silla observatory. The total timespan of all the observations for each star is much larger than the characteristic timescale of the measured photometric variations (see previous section). For our chemical analysis, we did not take into account the possible small temperature and gravity variations associated with the photometric variability. We discuss below the few cases where this negligence may matter.

The spectra before 1989 were recorded with the Reticon detector; for all the later observations the short camera of the CES spectrograph was mounted with an RCA CCD 1024x640 with 15μm^2 pixels, yielding a wavelength coverage between 35 Å in the blue and 70 Å in the red part of the spectrum.

The data were reduced using IHAP and MIDAS in a standard way. The wavelength calibration was performed after the extraction of the spectrum and was based on 15 to 40 thorium lines with a smooth dispersion curve; the rms deviation between the analytic curve and the line positions was typically less than 2 mÅ. Finally, a normalisation was performed by dividing the spectra by a smooth response (polynomial or spline) curve fitted to the continuum. The central wavelengths of the spectral lines were determined by gaussian fitting. The equivalent widths of single lines were computed by direct integration. For blends consisting of important lines the equivalent widths of the different components were computed by multiple gaussian fitting using the ALICE graphical user interface of MIDAS. A sample of the high quality spectra is shown in Fig. 1 and 3. The region around 4925 Å is very interesting as it contains lines of Fe I, Fe II, C I and Ba II. While the Fe I/Fe II linestrength ratio is a good model parameter estimator, the C and Ba lines are very useful to see the effects of possible dredge-ups.

4. Atmospherical parameters

One of the main problems in the chemical analysis of stars, is the accurate quantitative determination of the effective temperature and gravity.

The X and Y parameters of the Geneva photometric system can give us a first qualitative indication on the nature of the stars. X and Y are reddening independent parameters; X is mainly dependent on the effective temperature and Y on the gravity (Cramer and Maeder, 1979). In Fig. 2 we plotted the positions of the programme stars in the XY-diagram of the Geneva system together with theoretical positions for stars with different MK spectral type and solar composition. In Table 2 we give the mean X and Y values of each object. It is clear from Fig. 2 that the stars are indeed highly luminous and mainly from spectral type late A and early F. It seems that HD 95767, HD 108015, HD 112374 and HD 131356 are somewhat cooler than the other stars, which is also seen in Fig. 1 and Fig. 3.

Unfortunately the specific characteristics of the Geneva photometric system are not well suited here for quantitative model parameter estimates as most of the stars are too cold for a good calibration in terms of temperature and gravity.

Deducing the effective temperature and gravity from model fits through the optical part of the SED is hampered by the uncertainty of the total reddening (interstellar and circumstellar) and to a lesser extent the adopted metallicity. Those parameter estimates can thus again only be used as first estimates.

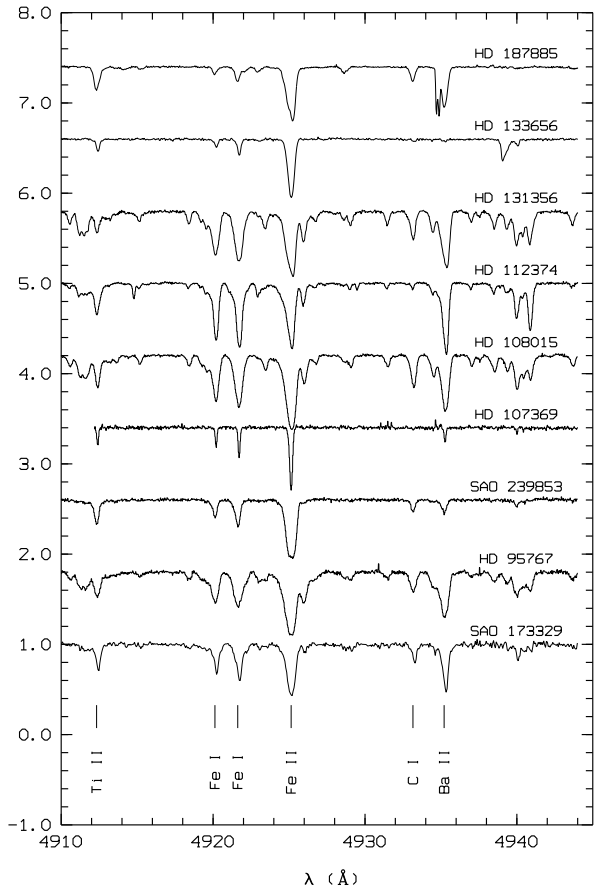

Fig. 1. Comparison between the normalized spectra around 4925 Å of the programme stars. The spectra are shifted so that the lines of the different stars have the same position.

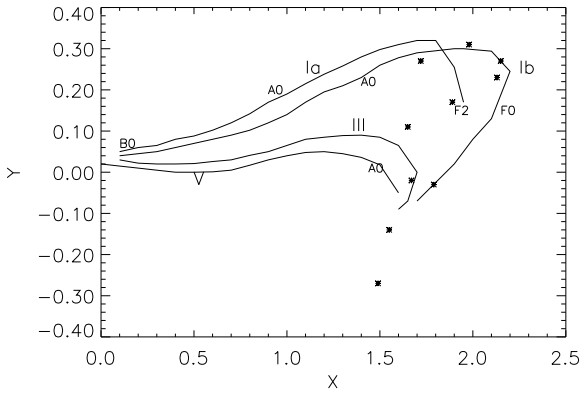

Fig. 2. Positions of the programme stars in the XY-diagram of the Geneva photometric system

Table 2. The XY values of the programme stars.

Nr.	Star	X	Y
1	SAO 173329	1.89	0.17
2	HD 95767	1.67	−0.02
3	SAO 239853	2.13	0.23
4	HD 107369	2.15	0.27
5	HD 108015	1.79	−0.03
6	HD 112374	1.55	−0.14
7	HD 131356	1.49	−0.27
8	HD 133656	1.98	0.31
9	HD 158616	1.65	0.11
10	HD 187885	1.72	0.27

A spectroscopic estimate for the temperature is found by the requirement that the abundance should be independent of the lower excitation potential of the lines of a certain element. This method is often used considering Fe I lines. It was, however, difficult to apply this method on our dataset, as one needs a good sample of lines with a large spread in excitation energy in order to average out the internal errors due to uncertain log(gf) values, errors in the equivalent width determination, etc.

An upper limit for the model temperature can be found by considering the absence or presence of He I lines in the spectral range covered, the solar helium content constituting a lower limit for the helium abundance. Unfortunately, the strongest line at 4471.50 Å is heavily blended by a Ti II line at 4470.86 Å, and therefore its identification is difficult. The He I line at 5876 Å is in a clear part of the spectrum and is thus better suited. We have definitely detected helium only for HD 133656 and, surprisingly, also for HD 187885 which is classified as a F2 supergiant. We will come back to this point later in the discussion. For the other stars for which we observed the spectral ranges of the strongest helium lines, an effective temperature of 7500 K can be considered as a reliable upper limit for the supergiants.

Starting from the photometric guess for the temperature and gravity, we derived the parameters for an appropriate model atmosphere by requiring that the different ions of the same element should yield the same abundance. We used only the iron lines for this ionisation balance, as it is the only element with enough lines of both ionisation stages. The non-LTE effects on iron lines are discussed by Brown et al. (1983) : these authors found that the Fe II lines are only affected by non-LTE effects at large equivalent widths while for Fe I the lines with small excitation potential are the most affected. The excitation potentials of the Fe I lines we used are most often larger than 2.5 eV, which implies that no large non-LTE effects are expected. Venn (1995a, 1995b) discussed in detail 22 A-F massive supergiants and concluded that the non-LTE effects on the Fe I lines are severe (0.2-0.3 dex), especially for the hotter objects. Boyarchuk et al. (1985) estimated the non-LTE effects on the Fe I abundance to be 0.2 for F0 supergiants but decreasing to about 0.03 for F8 supergiants. As our sample stars are cooler then the objects discussed by Venn and we limit ourselves to lines smaller then 100 mÅ, the non-LTE effects on the Fe I abondance are problably smaller then the 0.2 dex level.

If the constraint of the ionisation balance is used as model parameter estimator, we found that an increase of log(g) by 0.5 dex, corresponded with an increase of the effective temperature by 300-400 K.

Throughout our analysis we assumed that the microturbulent velocity (V_t) is independent of optical depth; we adopted a value of +5 km/s if there were not enough lines of the same element in the same ionisation stage to determine V_t independently. Such a determination of V_t is performed by forcing the abundance determination of the individual lines to show no dependence on equivalent width. We found this method only to be reliable if there are enough lines in the whole range of equivalent widths considered, because of the important uncertainties in the adopted log(gf) values. In any case, we only used lines with an equivalent width smaller that 150 mÅ in our chemical analysis, this in order to reduce the effect of uncertainty in the V_t value, damping parameter and possible non-LTE effects in the outer layers of the photosphere, where the stronger lines are formed. A V_t of 5 km/s is a reasonable estimate which emerged from our computations of stars with many lines and from the literature (e.g. Luck et al., 1990; Kodaira et al., 1970; Luck, 1993).

For every star, we will list the abundances for two parameter sets with a gravity difference of 0.5 dex, taking all model parameter indicators into account. This will give us some idea on the accuracy of our results. We will discuss the abundances of the stars individually, but first we comment on the error analysis.

4.1. Computational method and assumptions

Abundances of the chemical elements were computed in local thermodynamic equilibrium (LTE) using a standard model atmosphere analysis technique based on a code developed by Baschek et al. (1966) and later adapted by various people (e.g. Burger, 1976; Mulder, 1984; myself). The abundance of a certain element is computed through a match between the measured equivalent width and the equivalent width computed by integration through a model atmosphere using the abundance as a free parameter.

The model atmospheres with solar metallicities were taken from the model grid published by Kurucz (1979); in some cases interpolation in between several models was necessary. Models with lower metallicities or with parameters not included in the original grid, were computed using the ATLAS 8 code of Kurucz as described by Castelli (1988). To take the line-blanketing into account, we used line opacity distribution functions (ODF) with the appropriate metallicity and with microturbulent velocity V_t = 2 km/s.

The LTE model atmospheres are plane-parallel, with 40 homogeneous layers and in hydrostatic and radiative equilibrium.

For line identification we used mainly the line lists by Thévenin (1989, 1990) that are based on lines identified in the solar spectrum by Moore et al. (1966). For He, C, N and O line-identification we used the lists published by Lambert et al. (1982), Wiese et al. (1966) and Kodaira et al. (1970). The list of all the identified lines that were used in the chemical analysis calculations for every star can be obtained by the author (HVW) upon request.

The main sources for the fundamental data for the atomic lines (excitation potential and oscillator strength) are the two lists published by Thévenin (1989, 1990). Thévenin performed an inverted solar abundance analysis by comparing synthetic spectra with the solar atlas of Delbouille et al. (1973), using the solar abundances by Holweger and the solar model by Gustafsson (see Thévenin for references). By using the more accurate Holweger-Müller solar model, and his log(gf) values, he found good agreement between his computed solar abundances and the solar abundances as given by Grevesse (1989). We used the solar abundances by Grevesse as a reference. For the C, N, O line data, several sources are considered (see below).

5. Error analysis

5.1. Internal errors

A good indicator for the internal consistency of the analysis is given by the line-to-line scatter on the abundance for elements for which many lines were observed. In Tables 4–10 we list for every star and every ion the number of lines (N) used in the analysis and the standard deviation (σ) about the unweighted mean of the abundance calculations. One notes that the typical σ for species for which more than five lines were considered, is between 0.15 and 0.25 dex. For a Gaussian distribution the uncertainty on the mean is then expressed by ($\sigma/\sqrt{N}$). For species with less than five lines the standard deviation is not a good indicator for the internal error in the analysis.

For a good model atmosphere (in ionisation and excitation equilibrium) line-to-line scatter is mainly determined by $non\text{-}systematic$ errors in the equivalent width computation (estimated to be accurate at the 5-20 % level, depending on the signal-to-noise of the spectrum) and in the log(gf) values. Other contributors to the scatter could be differential non-LTE effects, non-detected blends, and, for the variable stars, the different photometric phases of the spectra.

5.2. Model parameters

Another important issue are the uncertainties on the model parameters and their influences on the abundances. The effects of changes in the parameters (T_{eff}, log(g), V_t, Z) of the model atmosphere are not independent : a change in one parameter generally induces a shift in another, so that the abovementioned spectroscopic requirements (e.g. ionisation balance) be fulfilled. A typical shift of 0.5 dex in the log(g) induces a temperature shift of 300-400 K, in order that the ionisation balance still be matched. In Table 3 we list the abundance calculation of HD 108015 for different models with independent shifts in the temperature (300 K), gravity (0.5 dex) and microturbulent velocity (1 km/s) in order to illustrate the effects of parameter uncertainties on the computed abundances. The temperature shift of 300 K has by far the largest influence on the abundances in this temperature and gravity domain. The neutral ions of elements with a low ionisation potential are most affected in the stars

Table 3. Parameter dependence of the abundances. The abundance per element are given for HD 108015 using our preferred model with T_{eff} = 7500 K; log(g) = 1.5 and V_t = 4 km/s, together with the differences when we induced independent shifts in T_{eff} of 300 K, log(g) of 0.5 dex and V_t of 1 km/s.

Ion	N	7000 1.5 4	7000 **1.0** 4	7000 **2.0** 4	**7300** 1.5 4	**6700** 1.5 4	7000 1.5 **5**
C I	6	8.64	−0.01	+0.03	+0.11	−0.07	−0.06
N I	2	8.18	−0.05	+0.04	+0.05	0.00	−0.06
O I	3	8.79	−0.06	+0.08	−0.03	+0.06	−0.05
Na I	2	6.62	+0.09	−0.09	+0.23	−0.20	−0.02
Si I	5	7.87	+0.12	−0.09	+0.26	−0.27	−0.04
S I	3	7.06	+0.03	−0.01	+0.19	−0.15	−0.02
Ca I	6	6.31	+0.12	−0.09	+0.30	−0.24	−0.01
Sc II	1	2.30	−0.13	+0.12	+0.18	−0.18	−0.03
Ti II	5	4.76	−0.13	+0.13	+0.15	−0.14	−0.11
V I	1	3.56	+0.05	−0.05	+0.37	−0.30	−0.02
V II	1	3.43	−0.12	+0.12	+0.15	−0.15	0.00
Cr I	7	5.73	+0.07	−0.05	+0.27	−0.22	−0.03
Cr II	1	5.71	−0.12	+0.12	+0.05	−0.03	−0.02
Mn I	6	5.22	+0.07	−0.06	+0.27	−0.24	−0.05
Mn II	3	5.71	−0.11	+0.11	+0.08	−0.07	−0.05
Fe I	52	7.57	+0.08	−0.06	+0.28	−0.23	−0.03
Fe II	8	7.58	−0.09	+0.10	+0.12	−0.10	−0.07
Ni I	16	6.36	+0.08	−0.06	+0.27	−0.22	−0.04
Ni II	1	6.36	−0.12	+0.13	+0.07	−0.07	−0.14
Zn I	2	4.44	+0.08	−0.06	+0.27	−0.23	−0.03

since these metals are mostly ionised and a small change in the ionisation fraction has much more influence on the computed abundances of the neutral lines than on the ionised ones. Note, however, that the abundance relative to Fe ([el/Fe]) is much less affected by uncertainties of the model parameters for these elements represented by neutral ions since the errors due to uncertainties on the model parameters largely cancel (see Table 3). Generally one can say that the ions with the smallest fraction are the most influenced by uncertainties on the ionisation balance induced by the errors on the temperature and gravity.

Although we limited ourselves to lines with an equivalent width smaller than 150 mÅ, the uncertainty on the microturbulent velocity can have important effects for species for which the mean equivalent width of all the used lines is large ($\geq$ 100 mÅ). For instance, the influence on the Ti II lines, which have a mean equivalent width of 110 mÅ, is considerable : a 1 km/s shift in V_t yields a 0.11 dex shift in the abundance.

Only for objects showing a severe iron deficiency ([Fe/H] $<$ -1) did we compute atmospherical models with an appropriate overall metallicity, using ATLAS 8. For the other stars we did not find a significant influence on the computed abundances of small changes in the overall metallicity of the model atmosphere.

5.3. Log(gf) values

We used mainly the log(gf) values by Thévenin (1989, 1990) for lines also observed in the Sun. These values are based on an inverted solar analysis and thus are dependent on the used solar model and abundance system. A different abundance for iron would affect the log(gf) values in a systematic way. In order to check our results for possible systematic effects we compared the log(gf) values of Thévenin with the literature compilation of oscillator strengths of Führ et al. (1988), which is another often used source. The mean on the difference of all the log(gf) values of the 85 common Fe I lines we used in our analysisis is -0.05 with a standard deviation of 0.16 (in this comparison we did not take into account the two lines with a difference of -0.70 and -0.84). Other ions for which no significant difference is found, are Cr I with 11 common lines and a mean difference of -0.05 with a rms of 0.12, Ti II with 30 shared lines and a mean difference of -0.02 but with a large scatter (rms = 0.26) and Ni I with 16 useful lines giving a mean difference of -0.08 and a rms of 0.14.

On the other hand, the Fe II lines seem to show a larger systematic effect : the 20 lines that are common to both lists (again after eliminating two lines with an abnormally strong disagreement) show a mean difference of -0.12 dex with a rms of 0.14, the values of Thévenin being the smallest. The 4 Cr II lines also show a large mean deviation of -0.17 with an rms of 0.09. Finally, the odd elements Sc and Mn also show rather large systematic differences : for the 4 Sc II lines a mean difference of -0.11 with a rms of 0.14 while the Mn I lines give a mean of -0.07 but a very large rms of 0.33.

Computing the Fe abundance of HD 108015 with the 38 common Fe I lines in the two sources of oscillator strength yielded no difference in internal scatter : for both sources the resulting rms on the computed abundance is 0.18; the difference on the mean amounts to 0.06 dex.

We used the log(gf) values by Thévenin for the elements Ca, Sc, Ti, V, Cr, Mn, Fe and Ni as this list is much more complete and we can thus achieve a better internal consistency. Comparing, however, our results with LTE analysis of stars using the values of Führ et al., we have to take these systematic effects into account. The scatter on the differences makes clear that a large part of the line-to-line scatter of the abundances are due to uncertain log(gf) values, and underscores the importance of good atomic data for stellar spectroscopy.

5.4. Individual species and non-LTE effects

Possible non-LTE effects are more difficult to quantify. By limiting our abundance analysis to lines with an equivalent width smaller than 150 mÅ, we focus on lines formed in deeper layers where the non-LTE effects are known to be smaller. Ideally one should use a full non-LTE, line-blanketed model atmosphere but such models are very difficult to compute. By all means, the non-LTE effects are not thought to be very large for Ib supergiants in this temperature domain (see e.g. Venn, 1993). We now give a small overview of the line-selection for the most important species and comment on possible systematic non-LTE effects. The main chemical indicators to probe for yields of stellar evolution are C, N, O, Fe and the s-process elements Sr, Y, Zr and Ba.

We used a wide variety of carbon lines in our analysis : the most important are the multiplets at 4770 and 7115 Å and the individual line at 6587.662 Å in the Hα region. The former

multiplet is for the cooler stars plagued with blends while the latter is in a clear part of the spectrum. We did not attempt to observe the forbidden line at 8727 Å. The log(gf) values we used for C I are mainly from Lambert et al. (1982) and were completed with values of Wiese et al. (1966) and Kurucz and Peytremann (1975). We found a good consistency between the different lines and different log(gf) sources so the internal accuracy of the C abundance is rather good. As can be seen from Table 3 the C abundance is not very sensitive to parameter uncertainties and for the weak lines the non-LTE effects are thought to be small in our temperature range even for supergiants (Venn, 1993, 1995a; Luck and Lambert, 1985).

The nitrogen lines used in our analysis are mainly from the multiplet at 8700 Å and the triplet at 7445 Å. Unfortunately, the mean equivalent width of these lines is rather large for stars that have solar or moderately deficient composition, so the N abundance is uncertain due to the dependence on the microturbulent velocity in these cases. Furthermore the non-LTE effects can be severe (e.g. Luck and Lambert, 1985; Venn, 1993, 1995a) in the sense that the LTE analysis yields a higher value for the N-abundance than the non-LTE calculations. Luck and Lambert (1985) showed that the non-LTE effects on the N I lines are, however, not very large (< 0.1 dex) for equivalent widths smaller than 100 mÅ in the temperature range from 6000 to 7500 K at gravities from 1.0 to 2.0. In absolute numbers, the LTE N-abundances are the most uncertain due to the large non-LTE effects.

Unfortunately, neutral oxygen does not show many useful lines in the optical part of the electromagnetic spectrum. The strong near-IR triplets at 7775 Å and 8446 Å are used as a luminosity indicator and their non-LTE effects are known to be severe (e.g. Luck et al., 1990). The line at 4386.30 Å is generally blended with the Ti II line at 4367.68 Å and is therefore not very useful to deduce the chemical content. Fortunately, most of the stars are hot enough as to show the triplet at 6150 Å (see Fig. 3). For the cooler stars, however, the triplet is blended with the Si I line at 6155.14 Å and the Fe I line at 6157.73 Å, which makes an accurate determination of the equivalent width difficult. Earlier sources give significantly dissimilar oscillator strengths for the triplet : Wiese et al. (1966) list -1.16, -0.73, -0.45 for the lines at respectively 6155.98, 6156.77, 6158.18 Å, but the values used by Lambert et al. (1982) -0.66, -0.44, -0.29 are now generally evaluated to be much better (e.g. Venn, 1993). We found the most consistent results with the 4386.3 Å line for the extremely metal deficient objects for which this line could be used. We did not use the forbidden [O I] lines at 6300 and 6363 Å.

The s-process element abundance determination is severely hampered by the lack of useful lines in the optical. The line of Sr II at 4215.54 Å is a resonance line and most often too strong to be valuable. The same applies to the Ba II resonance lines at 4554.04 and 4934.1 Å and also to the lines at 6141.73 and 6496.91 Å : these lines are only usable for the severely deficient objects. The higher excitation Ba II line at 4524.94 Å is only measured in one object but it is heavily blended there. For the moderately deficient stars we can only give a very rough indication of the abundance of the s-process elements as we did not observe weak enough lines. The log(gf) values are taken from the most recent compilation of Kurucz (1995) which we obtained via internet.

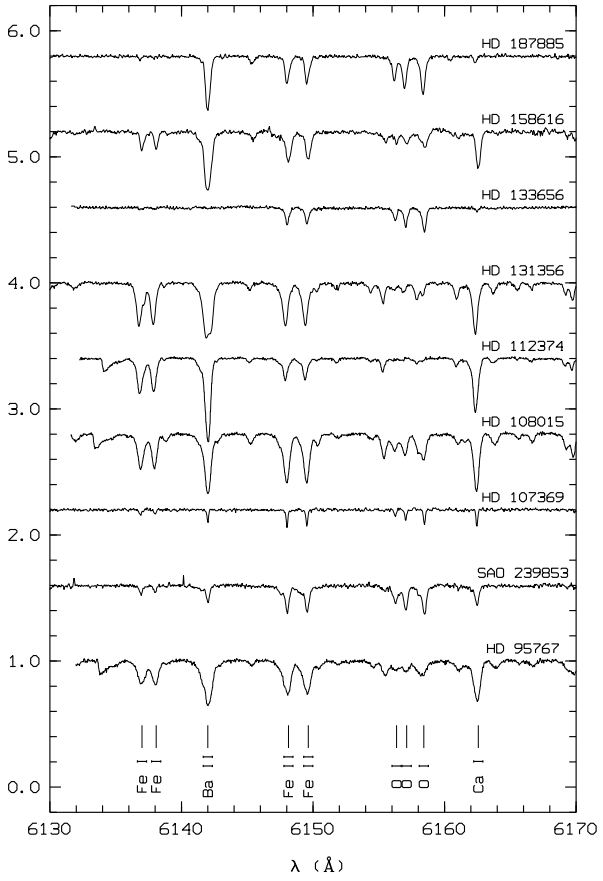

Fig. 3. Comparison between the normalized spectra around 6150 Å of the programme stars. The spectra are shifted so that the lines of the different stars have the same position.

6. Chemical analysis

In the Tables 4 to 10 we give the result of the abundance analysis of every object, absolute and relative to the solar value, together with the number of lines used, the mean equivalent width of the lines and the internal scatter. A detailed list of the equivalent width of the individual lines used in the analysis of each star, together with the atomic data and the reference of the log(gf)-values, can be obtained by the author upon request.

In Fig. 1 and 3 we show the spectral region around 4925 Å repectively 6150 Å of the programme stars to illustrate the abundance results. The first spectral region is interesting as it contains beside Fe I and Fe II lines also the C I line at 6932 Å and the Ba II 4934 Å line. The second region shows besides the O I triplet also Fe I, Fe II, Ca I and Ba II lines.

Table 4. Chemical analysis of the programme stars. For every star, the analysis is given for two model atmospheres of which the effective temperature and gravity are given in-between brackets. For every ion, the number of used lines are given together with the mean equivalent width. For every model, we list the mean absolute abundance, the abundance relative to the solar value and the internal scatter if more than one line is used.

SAO 173329 V_t = 5 km/s			Model 1 (7000,1.5)			Model 2 (6500,1.0)		
Ion	N	$\overline{W_\lambda}$	A	[el/H]	σ	A	[el/H]	σ
C I	6	46	8.01	−0.55	0.10	7.87	−0.69	0.10
N I	4	70	7.54	−0.51	0.23	7.57	−0.48	0.24
S I	6	26	6.50	−0.71	0.10	6.29	−0.92	0.17
Ca I	1	107	5.56	−0.80		5.21	−1.15	
Ti II	8	78	4.30	−0.69	0.18	3.93	−1.06	0.17
Cr I	2	14	5.17	−0.50	0.06	4.86	−0.81	0.07
Cr II	1	140	5.27	−0.40		5.03	−0.64	
Mn I	3	35	4.37	−1.02	0.07	4.01	−1.38	0.08
Fe I	11	54	6.85	−0.82	0.18	6.51	−1.16	0.20
Fe II	3	53	6.83	−0.84	0.37	6.49	−1.18	0.41
Ni I	2	29	5.29	−0.96	0.01	4.94	−1.13	0.04
Zn I	1	28	3.77	−0.83		3.42	−1.18	

Table 5. Continuation table 4

HD 95767 V_t = 5 km/s			Model 1 (7600,2.0)			Model 2 (7000,1.0)		
Ion	N	$\overline{W_\lambda}$	A	[el/H]	σ	A	[el/H]	σ
C I	5	83	8.63	+0.07	0.07	8.39	−0.17	0.07
N I	2	146	8.02	−0.03	0.05	7.94	−0.11	0.05
O I	3	59	8.55	−0.38	0.08	8.49	−0.44	0.08
Na I	2	42	7.09	+0.76	0.18	6.81	+0.48	0.19
Si I	3	32	7.78	+0.23	0.04	7.53	−0.02	0.03
S I	8	43	7.22	+0.01	0.11	6.95	−0.25	0.13
Ca I	4	36	6.60	+0.24	0.15	6.24	−0.12	0.16
Ti II	6	90	4.88	−0.11	0.18	4.35	−0.64	0.20
Cr I	2	27	5.87	+0.20	0.11	5.54	−0.13	0.10
Mn I	5	61	5.62	+0.23	0.19	5.23	−0.16	0.22
Mn II	1	84	6.08	+0.41		5.75	+0.36	
Fe I	37	47	7.77	+0.10	0.27	7.40	−0.27	0.27
Fe II	3	47	7.83	+0.16	0.23	7.44	−0.23	0.30
Ni I	11	40	6.51	+0.26	0.27	6.17	−0.08	0.24
Zn I	1	46	4.48	−0.12		4.09	−0.51	

Table 6. Continuation Table 4

SAO 239853 V_t = 5 km/s			Model 1 (7500,1.0)			Model 2 (7200,0.5)		
Ion	N	$\overline{W_\lambda}$	A	[el/H]	σ	A	[el/H]	σ
C I	7	43	8.17	−0.39	0.13	8.06	−0.50	0.13
N I	6	71	7.77	−0.28	0.16	7.75	−0.30	0.16
O I	4	73	8.71	−0.22	0.09	8.69	−0.24	0.08
Mg II	1	60	7.18	−0.40		7.18	−0.40	
Si I	2	20	7.24	−0.31	0.18	7.14	−0.41	0.16
S I	6	22	6.81	−0.40	0.16	6.70	−0.51	0.17
Ca I	4	45	5.88	−0.48	0.10	5.72	−0.64	0.10
Sc II	1	24	1.99	−1.11		1.70	−1.40	
Ti II	17	84	4.45	−0.54	0.17	4.20	−0.79	0.17
Cr II	3	76	4.86	−0.81	0.20	4.66	−1.01	0.19
Fe I	23	44	6.83	−0.84	0.23	6.64	−1.03	0.22
Fe II	15	45	6.90	−0.77	0.17	6.72	−0.95	0.15
Ni I	2	19	5.45	−0.80	0.05	5.30	−0.95	0.05
Ni II	1	40	5.41	−0.84		5.23	−1.02	
Zn I	1	11	3.87	−0.73		3.70	−0.90	
Zr II	2	16	1.58	−1.02	0.04	1.30	−1.30	0.06
Ba II	2	53	1.00	−1.13	0.40	0.68	−1.45	0.68

Table 7. Continuation Table 4. The Carbon abundance is an upper limit

HD 107369 V_t = 2.5 km/s			Model 1 (8000,2.0)			Model 2 (7200,1.0)		
Ion	N	$\overline{W_\lambda}$	A	[el/H]	σ	A	[el/H]	σ
C I	1	**5**	**7.29**	**−1.27**		**6.94**	**−1.62**	
N I	8	41	7.37	−0.68	0.25	7.26	−0.79	0.24
O I	3	16	7.83	−1.10	0.02	7.77	−1.16	0.02
Si II	1	75	6.60	−0.95		6.38	−1.17	
S I	2	11	6.32	−0.95	0.09	5.94	−1.27	0.08
Ca I	1	23	5.62	−0.74		4.99	−1.37	
Sc II	1	6	1.94	−1.16		1.20	−1.90	
Ti II	9	45	4.15	−0.84	0.09	3.49	−1.50	0.09
Cr II	2	50	4.61	−1.06	0.06	4.11	−1.56	0.07
Fe I	8	15	6.61	−1.06	0.08	6.01	−1.66	0.06
Fe II	6	36	6.55	−1.12	0.06	6.02	−1.65	0.08
Ba II	3	25	0.95	−1.18	0.13	0.03	−2.10	0.14

6.1. Results on individual objects

6.1.1. SAO 173329

This rather faint star is not yet very well covered by our spectra : we more precisely lack O I lines and more good Fe II lines for the spectroscopic parameter determination.

Irrespective on the precise model parameters, the star is metal deficient with [Fe/H] = −0.8 to −1.1 respectively for the hotter and cooler model proposed. C and N seem to be overabundant relative to Fe, with [C/Fe] = +0.3 and [N/Fe] = +0.3. The iron peak elements Mn, Ni and Zn follow the Fe deficiency well. Cr turns out to be slightly overabundant relative to Fe [Cr/Fe] = +0.3; this result is based on only three lines of two ionisation stages. SAO 173329 is a metal deficient object for which more data are needed.

6.1.2. HD 95767

The energy distribution of this object is well fitted with a model atmosphere of 7500 K and log(g) = 2.5 (Bogaert, 1994). For this temperature we found however that log(g) = 2.0 using the ionisation balance on Fe lines as the only criterion. The Fe I abundance determination is well documented with 11 lines but the Fe II abundance relies on only 3 lines. A lower log(g) of 1.0 yields an effective temperature of 7000 K.

The composition of this star turns out to be solar within the errors of the analysis. Only the O I abundance, based on the triplet at 6150 Å seems to be remarkably low. The two Na I lines give a high and even suprasolar abundance. Overabundances of sodium are also observed in massive A-F supergiants, and are

Table 8. Continuation Table 4.

HD 108015 V_t = 4 km/s			Model 1 (7000,1.5)			Model 2 (6600,1.0)		
Ion	N	$\overline{W_\lambda}$	A	[el/H]	σ	A	[el/H]	σ
C I	5	96	8.60	+0.04	0.12	8.48	−0.08	0.12
N I	2	92	8.18	+0.13	0.08	8.14	+0.09	0.08
O I	3	77	8.79	−0.14	0.09	8.80	−0.13	0.09
Na I	2	30	6.62	+0.29	0.06	6.41	+0.08	0.06
Si I	5	67	7.84	+0.29	0.18	7.65	+0.10	0.16
S I	3	42	7.06	−0.15	0.12	6.87	−0.34	0.12
Ca I	6	40	6.31	−0.05	0.17	6.07	−0.29	0.18
Sc II	1	61	2.30	−0.80		1.94	−1.16	
Ti II	4	112	4.73	−0.26	0.14	4.43	−0.56	0.14
V I	1	40	3.56	−0.44		3.21	−0.79	
V II	1	14	3.43	−0.57		3.12	−0.88	
Cr I	7	52	5.60	−0.07	0.20	5.35	−0.32	0.22
Cr II	1	40	5.71	+0.04		5.56	−0.11	
Mn I	6	62	5.29	−0.10	0.29	5.02	−0.37	0.30
Mn II	3	70	5.71	+0.32	0.15	5.52	+0.19	0.19
Fe I	50	51	7.57	−0.10	0.19	7.31	−0.36	0.20
Fe II	7	75	7.59	−0.08	0.20	7.35	−0.32	0.22
Ni I	15	45	6.35	+0.10	0.20	6.12	−0.13	0.21
Ni II	1	135	6.36	+0.11		6.15	−0.10	
Zn I	2	49	4.44	−0.16	0.07	4.19	−0.41	0.11

Table 9. Continuation Table 4

HD 131356 V_t = 6 km/s			Model 1 (6000,1.0)			Model 2 (6300,1.5)		
Ion	N	$\overline{W_\lambda}$	A	[el/H]	σ	A	[el/H]	σ
C I	11	93	8.18	−0.41	0.15	8.24	−0.32	0.15
N I	4	82	7.85	−0.20	0.18	7.82	−0.23	0.17
O I	3	27	8.29	−0.64	0.10	8.29	−0.64	0.10
Na I	2	41	6.13	−0.20	0.06	6.27	−0.06	0.06
Mg I	1	35	7.94	+0.36		8.09	+0.51	
Mg II	1	30	7.24	−0.34		7.23	−0.35	
Si I	2	41	6.99	−0.56	0.17	7.11	−0.44	0.18
S I	5	42	6.60	−0.61	0.15	6.71	−0.50	0.15
Ca I	6	40	5.33	−1.03	0.20	5.51	−0.85	0.19
Ti II	5	98	3.88	−1.11	0.22	4.14	−0.85	0.24
V I	1	50	2.67	−1.33		2.95	−1.05	
Cr I	6	39	5.29	−0.38	0.19	5.47	−0.20	0.19
Mn I	2	68	5.16	−0.23	0.26	5.35	−0.04	0.26
Fe I	49	57	6.89	−0.78	0.23	7.10	−0.57	0.23
Fe II	8	40	6.93	−0.74	0.19	7.09	−0.58	0.20
Ni I	11	59	5.76	−0.49	0.29	5.96	−0.29	0.29
Ni II	1	67	5.35	−0.90		5.52	−0.73	
Zn I	2	89	4.04	−0.56	0.19	4.24	−0.36	0.15

not well understood : it can be due to non-LTE effects but also due to deep mixing of synthesized Na from the proton capture reaction NeNa (Venn, 1995b and references therein).

We can conclude that the star has solar abundances within the errors, with only a low oxygen content and a high Na content. These abundances are also observed in pop. I supergiants (Luck and Lambert, 1985 and Venn 1995b respectively). In fact, HD 95767 is the only star in our sample which is located in the galactic plane. It probably is a genuinely massive supergiant, and its IR excess is then not the result of post-AGB evolution.

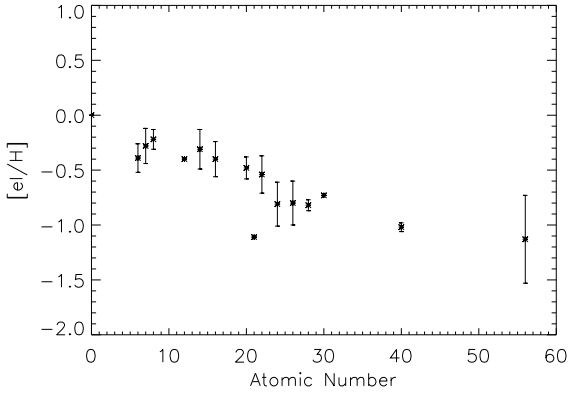

Fig. 4. The photospheric abundances of SAO 239853 relative to the solar values.

Table 10. Continuation Table 4

HD 158616 V_t = 5 km/s			Model 1 (7400,0.5)			Model 2 (7700,1.0)		
Ion	N	$\overline{W_\lambda}$	A	[el/H]	σ	A	[el/H]	σ
C I	8	56	8.50	−0.06	0.15	8.66	+0.10	0.15
N I	5	81	7.63	−0.42	0.21	7.67	−0.38	0.21
O I	4	62	8.40	−0.53	0.12	8.43	−0.50	0.12
Si I	1	19	7.53	−0.02		7.71	+0.16	
S I	9	33	7.13	+0.01	0.10	7.31	+0.10	0.09
Ca I	4	42	6.37	+0.01	0.21	6.63	+0.27	0.20
Sc II	1	28	3.29	+0.19		3.61	+0.51	
Ti II	2	49	4.70	−0.29	0.23	5.01	+0.02	0.23
Cr I	2	31	5.26	−0.41	0.02	5.54	−0.13	0.02
Cr II	2	69	5.30	−0.37	0.01	5.53	−0.14	0.00
Fe I	14	46	7.02	−0.65	0.34	7.29	−0.38	0.33
Fe II	10	63	6.96	−0.71	0.24	7.18	−0.51	0.24
Ni I	2	37	5.91	−0.29	0.16	6.14	−0.11	0.15
Ni II	1	66	5.63	−0.62		5.83	−0.42	
Zn I	1	25	4.40	−0.20		4.64	+0.04	
Y II	1	**186**	**2.77**	**+0.53**		**3.12**	**+0.88**	
Zr II	5	79	3.06	+0.46	0.20	3.36	+0.76	0.20

6.1.3. SAO 239853

This star is metal-deficient with an Fe abundance between -0.8 and -1.0 for the two proposed models. The atmosphere is C and N rich, with a [C/Fe] = +0.4, and [N/Fe] = +0.5. SAO 239853 displays products of the CN cycle and He burning products. The O abundance of [O/Fe] = +0.6 to +0.7 is about 0.2 dex higher than expected for an unevolved object with a [Fe/H] between −0.8 to −1.0 and may indicate a slight O enrichment. The only information we have concerning the s-process elements are two small lines of Zr and two lines of Ba. They yield a [s/Fe] between −0.3 and −0.4, which indicates a s-process element deficiency as observed also in other metal poor objects (Fig. 4).

6.1.4. HD 107369

HD 107369, the only star of our sample with neither Hα emission nor observed IR excess, does also display unique abundance patterns among our sample of stars. For the model parameters proposed by Kodaira and Philip (1984), we found a good

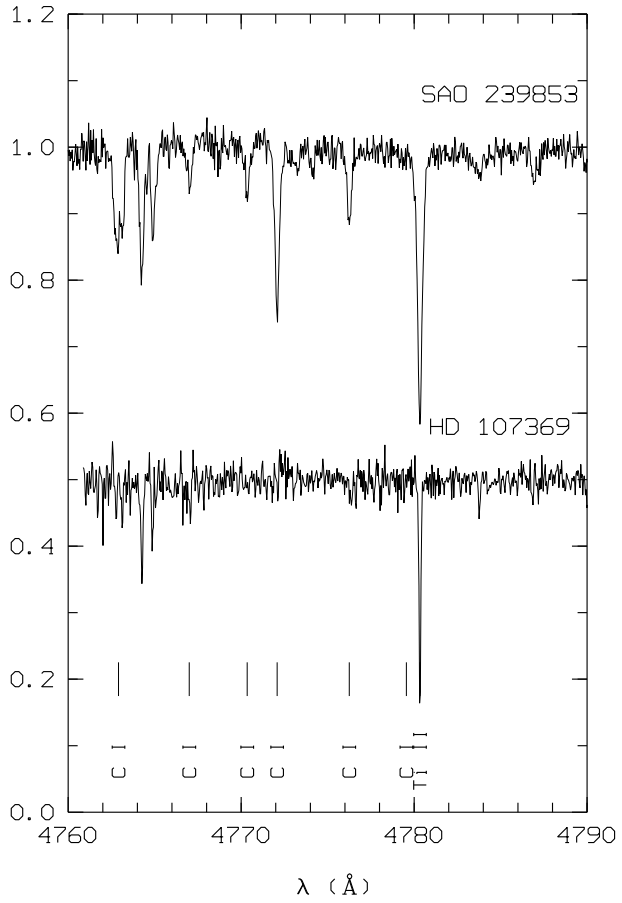

Fig. 5. Comparison between the spectra of HD 107369 and SAO 239853 of the region around the C mutiplet number 6.

match between the abundances based on the Fe I and Fe II lines. Unlike Kodaira and Philip, we found the star to be severely deficient ([Fe/H] = -1.1). Unfortunately, there is no line in common between both studies. The Fe-group, alpha-elements, Sc and the s-process elements follow the Fe depletion well.

The most remarkable observational characteristic of this object is, in our opinion, that the strong C I line at 4771.7 Å is not detected (Fig. 5). For an upper limit of 5 mÅ for this rather strong optical C line, we deduce an upper limit of the C abundance of 7.3 for model 1 (T_{eff} = 8000, log(g) = 2.0), or [C/H] < -1.3. For a cooler model, the situation is even more extreme, with [C/H] < -1.6. The N and O abundances, [N/H] = -0.7, [O/H] = -1.1 are less affected by model parameter changes. HD 107369 is the only star in our sample with such CNO abundance ratios. The object shows very clearly the yields of CNO-hydrogen burning on its surface : a N overabundance coupled with a C deficiency. There is no evidence for a third dredge-up in our spectra (see Fig. 6).

6.1.5. HD 108015

This star is very well covered with our spectra. The photometry indicates a temperature of 7000 K and a log(g) of 1.5. For this

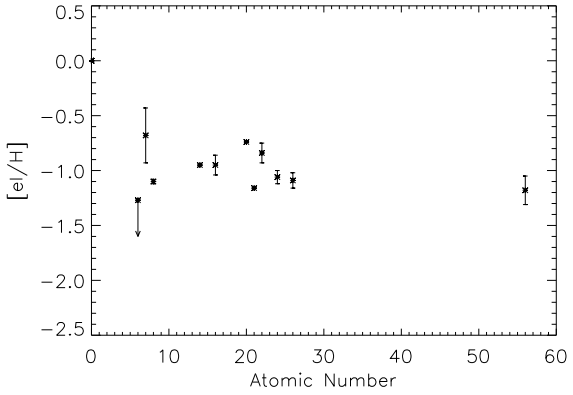

Fig. 6. The photospheric abundances of HD 107369 relative to the solar values.

model numerous Fe lines (50 Fe I lines and 7 Fe II lines) are also in ionisation balance. For the other elements represented by different ionisation stages (V, Cr, Ni) the abundances of the ions differ all by less than 0.15 dex. On the other hand, the Mn II lines give a significantly larger abundance than the Mn I lines. The same problem occurs in HD 95767 for the common Mn II line. This is probably an artifact from the analysis, as we have not accounted for broadening by hyperfine structure in our analysis of the strong Mn lines. Moreover, the Mn abundance is only based on a few lines, so an error in the log(gf) value or an undetected blend can influence the mean abundance significantly. We computed also the abundances for a cooler model (T_{eff} = 6600, log(g) = 1.0).

For our preferred model, the abundances of all but a few elements fall within 0.3 dex from the solar value. Exceptions are Sc (based on only one line), the abovementioned Mn II, and V. Note that, since we did not take broadening by hyperfine splitting into account, the abundance of especially Mn and Sc are upperlimits. The N abundance might be slightly suprasolar, but we note that our determination is only based on two lines. The O lines around 6155 Å (Fig. 1) are strongly blended with the Si I line at 6155.14 Å and the Fe I line at 6157.73 Å.

For our cooler model the Fe abundance is 0.3 dex less than the solar value. The CNO abundances are hardly affected by the model parameter changes.

6.1.6. HD 112374

The chemical composition of HD 112374 (HR 4912), the coolest star in our sample, was studied already in great detail by Luck at al. (1983). This star is also a photometric variable and is named LN Hya. The variability affects the line strength : slightly different equivalent widths were reported by Luck et al. for spectra taken at different epochs. Luck et al. used different atmospheric parameters for their two datasets, with the same temperature (6000 K) but different log(g) : 0.4 and 0.8. Note that HD 112374 is the only star in the sample for which the O triplet is not observed and that the Fe I to Fe II linestrength ratio also indicates a cooler supergiant than all other programme stars

(Fig. 1). We did not cover enough spectral intervals to perform an independent abundance analysis.

The analysis by Luck et al. (1983) shows the star to be metal deficient ([Fe/H] = −1.2) with the CNO abundances pointing towards an evolved object with a strong N ([N/Fe] = +0.5) enrichment as a product of the CN cycle. Neither a significant C enrichment ([C/Fe] = +0.1) nor a significant s-process elemental enrichment ([s/Fe] ≈ 0.0) is observed.

6.1.7. HD 131356

This object is an RV Tauri-type pulsating variable and is named EN TrA. The variations of the photospheric parameters which cause the photometric variability (Δm_v = 0.6 mag) also affect the line strengths. The C I line near Hα has been measured seven times : the mean equivalent width is 108 mÅ, the rms is 19 mÅ; extreme values are 143 and 87 mÅ. Ideally one should observe as broad a spectral region as possible during the same night in order to be fully consistent. Our spectra are, however, spread over a long time-interval and are analysed with only one average photospheric model.

The colours are very similar to those of HR 4912 : in the XY diagram we find HR 4912 and HD 131356 at the same locus. We computed the photospheric abundances for two model parameter sets with log(g) 1.0 and 1.5, corresponding to a T_{eff} of respectively 6000 and 6300 K. The star is moderately metal deficient with [Fe/H] = −0.7 to −0.5. O follows the Fe depletion rather well while C and N are mildly overabundant relative to Fe with respectively [C/Fe] = +0.3 and [N/Fe] = +0.6 to +0.3. For the other elements, only for S I, Ti II, Cr I and Ni I are the abundances determined from several lines, measured at different photometric epochs. The α elements follow the Fe depletion rather well. The Mg abundance is rather high, but it is based on only one line of each the neutral and single ionised ion with rather poor correspondence. Also the iron-peak elements follow the depletion, except for Cr (6 lines) and Mn (2 lines) which are overabundant relative to Fe. The detected Ba lines are too strong for abundance calculation purposes.

6.1.8. HD 133656

This object belongs to the hotter objects in our sample. The photometry, IUE spectrum, Hγ and Hβ line profiles all agree very well with an effective temperature of about 8000 K and a log(g) of 1.0. The match between the Fe I and Fe II abundances yields a temperature of 7800 at this gravity. For a detailed discussion on the abundances (see Fig. 7), we refer to Van Winckel et al. (1996b).

This star is metal poor ([Fe/H] = −1) but evolved, as indicated by the C and N abundances : [C/Fe] = +0.3, [N/Fe] = +0.7. With a [O/Fe] = +0.5, the O abundance follows the oxygen content of unevolved stars of the same metallicity. The light α-elements (Mg, Si, S) yield a [α/Fe] = +0.45, again a value as predicted by the chemical evolution of our Galaxy. The heavier α-element Ca seems to follow the Fe deficiency, and so do the Fe-peak elements Sc, Ti, Cr and Ni. The most remarkable fact

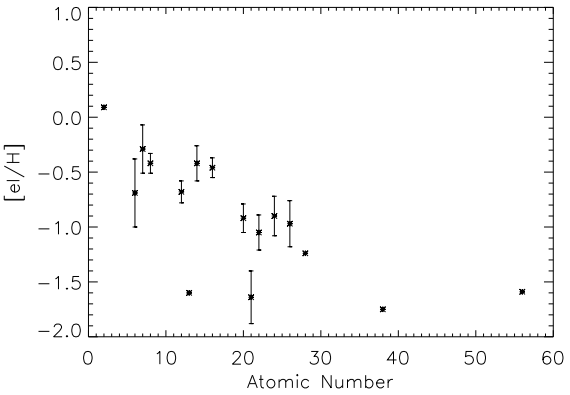

Fig. 7. The photospheric abundances of HD 133656 relative to the solar values.

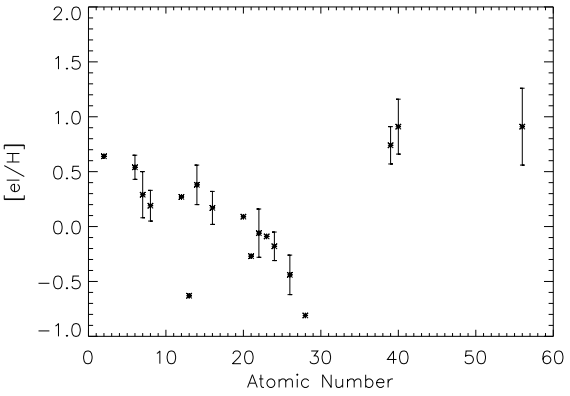

Fig. 8. The photospheric abundances of HD 187885 relative to the solar values.

is, however, that we have good evidence that the s-process elements Sr and Ba are deficient, relative to the iron abondance. This is illustrated in Figs. 1 and 3, were one can see that neither of the two Ba II lines at 4934 and 6142 Å are detected.

6.1.9. HD 187885

The chemical composition of this star was extensively studied by Van Winckel et al., 1996. The star in metal deficient ([Fe/H] = −0.5) and as can be seen on Fig. 8 the star fulfils all the chemical requirements of a prototypical post-AGB of post third dredge-up star : a supra solar helium content, a high C/O ratio and, above all, clear s-process enrichement.

6.1.10. HD 158616

A similar star to HD 187885 seems to be HD 158616, but unfortunately for this fainter star the quality of our data is not as good as for HD 187885.

The star is somewhat cooler than HD 187885 and our best estimate of T_{eff} is 7400 K with a log(g) of 0.5. We point out that the internal errors on the abundances of the Fe lines are rather large due to the fact that the spectroscopic measurements

were taken irrespecitive of the photometric phase: photometric variations with a total amplitude of 0.16 mag in the Geneva v-band are observed (Bogaert, 1994). The Fe I and the Fe II lines are well covered.

This star is mildly iron-deficient independent of the uncertainties on the model parameters.

The final analysis reveals some strong arguments for the similarity between HD 187885 and HD 158616 : the C abundance, with 8 lines among which the triplet of 7115 Å, is well defined and is high indeed. The C/O ratio is significantly higher than solar: for our preferred model, the carbon lines yield an abundance of 8.5, while the oxygen triplet gives 8.4. The latter value is uncertain due to severe blending.

The Ba II lines at 6141 (see Fig. 3) and 6497 Å are very strong, with equivalent widths of respectively 319 and 323 mÅ, so that the abundance determination critically depends on the adopted microturbulent velocity. For any reasonable velocity, however, a suprasolar Ba abundance is found; for V_t = 5 km/s it amounts to [Ba/H] = +1.4. The best lines to get reliable information on the s-process elemental abundances are the Zr II lines at 4359 (mildly blended with a Cr I line), 4371 (strongly blended with the C I line) and the doublet at 5350 Å. They imply a suprasolar Zr abundance which amounts to [Zr/Fe] = +0.46. The Y abundance is as yet highly uncertain as it is only based on one strong line with an equivalent width of 186 mÅ.

Unlike in the case of HD 187885, the S abundance of HD 158616 seems to be rather high compared to Fe with [S/Fe] = +0.7. It is based on the faint triplets at 4695 and 6757 Å and the blend at 8694 Å. Also the only Sc line leads to a, albeit very uncertain, high abundance.

Also the abundance analysis of HD 158616 clearly indicates previous AGB evolution and this as yet poorly studied star deserves further research.

7. Discussion

In Table 11 we list a synopsis of our abundance analyses. We give first the Fe abundance relative to the solar value followed by the abundances of C, N, O : these are the most important signatures of internal nucleosynthesis and dredge-up phenomena. When available, S and the mean of the α-elements Mg, Si, Ca and Ti abundances–listed as [α/Fe]–are given separately to show whether the S abundance behaves differently; next, the mean abundance of the available s-process elements (Sr, Y, Zr and Ba) relative to Fe is given. In the second part of the Table, we mention the results of the analyses of some objects from the literature, chosen as representative of classes of objects : HD 161796, HR 6144, 89 Her, HR 7671, HD 56126, HD 46703 are high-latitude F-supergiants; LS IV-12°111, PHL 174 are B stars at high galactic latitude thought to be in a post-AGB evolutionary state, the latter being markedly cooler than the former one; ROA 24 (HD 116745), V1, V29 are UV-bright supergiants in the globular cluster ω Centauri; K 648, DDDM-1 and BD+33°2642 are halo Planetary nebulae, and finally RU Cen is a relatively warm (T_{eff} = 6000) RV Tauri star. Note that for HR 6144, Venn (1995b) found different abundances pointing to a pop I nature of the star. The references for the LTE abundance analyses are also given.

The first characteristic to note is that our programme stars are most often significantly metal deficient, with HD 95767 and HD 108015 as noticeable exceptions. This result is a strong indication that our sample indeed consists of an old and hence low-mass population. The abundances and the low galactic latitude of HD 95767 (b = +2°) hints to a massive population I nature of the object. On the other hand, the galactic latitude of HD 108015 (b = +15°) is large for a population I supergiant.

The computed CNO abundance ratios, tracers of mixing of CNO-cycled and/or helium burning products, are also a good indication for the population of our sample stars. Indeed, evolved pop. I supergiants, in which the CN abundance ratios are mainly determined by the CN cycle of the CNO hydrogen combustion, have the following mean abundance ratios : [C/Fe] = -0.5, [N/Fe] = +0.5 and [O/Fe] = -0.3 (Luck and Lambert, 1985; Luck, 1993). The mild O deficiency of pop. I supergiants is not well understood : theoretical evolutionary calculations do not predict the convection to reach the deeper layers where the ON cycle occurs (Iben and Renzini, 1983). It is clear from Table 11 that our programme stars show significantly different CNO ratios from those of evolved population I supergiants. We repeat once more that the C, N, O abundance ratios relative to one another are not very model parameter dependent.

From the Fe-deficiency and the CNO abundance ratios one can thus conclude that our stars (except for HD 95767 and maybe HD 108015) indeed are low-mass objects in a late stage of stellar evolution.

It is remarkable that in our sample of stars only two objects clearly display the predicted chemical characteristics of stars that underwent the third dredge-up : HD 187885 and HD 158616 display a strong C enrichment with the C/O ratio respectively 1 and 2. N is enhanced in both stars but O only seems to be enhanced in the former star. With the detection of a He I line in HD 187885, we have a good indication that this star is He enriched. The most striking evidence for mixing of helium burning products in the atmospheres of these two stars comes however from the detection of large s-process elemental abundances. Indeed, with a [s/Fe] of +1.2 and +1.3 respectively, there can be no doubt that the s-process elemental abundances are strongly enhanced in these stars. Note that HD 158616 is as yet less well covered than HD 187885, and deserves further detailed attention.

The abundance patterns of HD 187885 and HD 158616 are very similar to those of HD 56126 as described by Klochkova (1995). Also for this metal deficient ([Fe/H] = -1.2), high velocity (V_{rad} = 91 km/s) object, large s-process elemental overabundances are found in combination with large C, N and O overabundances. The claim by Parthasarathy et al. (1992), that S is overabundant relative to the other α-elements in HD 56126 is not supported by the much more detailed analysis of Klochkova, and we will addopt the result of the latter author in the further discussion.

HR 7671 could be a similar object, but as seen in Table 11 this star displays peculiar CNO abundances with strong C and

Table 11. Synopsis of the abundance analyses of our sample stars supplemented with information of related objects taken from the literature. [α/Fe] is the mean of the abundances of the α-elements Mg, Si, Ca and Ti as far as available. [s/Fe] is the mean of the abundances of the s-process elements Sr, Y, Zr and Ba as far as available.

Star	[Fe/H]	[C/Fe]	[N/Fe]	[O/Fe]	[S/Fe]	[α/Fe]	[s/Fe]	S
SAO 173329	−0.8	+0.3	+0.3		+0.1	+0.1		
HD 95767	+0.1	−0.1	−0.2	−0.5	−0.1	0.0		
SAO 239853	−0.8	+0.4	+0.6	+0.8	+0.4	+0.4	−0.4	
HD 107369	−1.1	<−0.2	+0.4	0.0	+0.1	+0.2	−0.1	
HD 108015	−0.1	+0.1	+0.2	−0.1	−0.1	+0.1		
HD 112374	−1.2	+0.1	+0.5	+0.8	+0.1	+0.2	−0.3	1
HD 131356	−0.6	+0.3	+0.3	−0.1	+0.1	0.0		
HD 133656	−0.7	+0.2	+0.5	+0.6	+0.4	+0.2	−0.4	
HD 158616	−0.7	+0.6	+0.3	0.0	+0.7	+0.6	+1.2	
HD 187885	−0.4	+1.0	+0.7	+0.6	+0.6	+0.6	+1.3	
HD 161796	−0.3	+0.3	+1.1	+0.4	+0.7	+0.2	0.0	2
HR 6144	−0.4	+0.3	+0.9	+0.3	+0.4	+0.4	+0.2	2
89 Her	−0.4	+0.3	+0.6	+0.1	+0.1	+0.1	0.0	2
HR 7671	−1.1	−0.3	+0.1	−0.3	+0.3	+0.2	+0.6	2
HD 56126	−1.2	+1.2	+1.1	+0.7	+0.8	+1.2	+2.2	3
HD 46703	−1.6	+1.1	+1.7	+1.1	+1.3	−0.5	−0.7	10
LS IV−12°111	<−1.0	−0.9	+0.7	+0.8	+0.4	+0.8		4
PHL 174	<−0.5	−1.9	−0.8	−0.6		−0.7		4
ROA 24	−2.1	+0.6	+1.8	+1.3	+0.7	+0.5	+0.3	5
V 1	−1.8	+0.7		+1.1	+0.9	+0.5	+0.6	5
V 29	−2.0	+0.2		+1.1		+0.6	+0.4	5
K 648*	−2.3	+2.4	+0.8	+1.1	+0.3			6
DDDM−1*	−0.9	<−0.6	+0.3	+0.1	+0.2			7
BD+33°2642	−2.0	−1.1	−0.7	−0.8		−1.0		8
RU Cen	−1.4			+1.4			+0.3	9

1) Luck et al., 1983
2) Luck et al., 1990
3) Klochkova, 1995
4) Conlon et al., 1993
5) Gonzalez and Wallerstein, 1994
6) Adams et al., 1984
7) Clegg et al., 1987
8) Napiwotzki et al., 1994
9) Luck and Bond, 1989
10) Bond and Luck, 1987
∗ Ar is used as metallicity indicator.

minor N depletion; it also has a high Li abundance of [Li/H] = +1.4. The nature of this peculiar object is still a matter of debate, certainly as no IR excess due to circumstellar material is detected (Trams et al., 1991).

To our knowledge HD 187885, HD 158616 and HD 56126 are the only known high galactic latitude field supergiant with such clear-cut abundance patterns pointing to previous AGB evolution. They display a wide spread in metallicity : [Fe/H] is respectively −0.5, −0.5 and −1.2.

In the globular cluster ω Centauri, however, there are 3 UV-bright stars (see Table 11) that also display s-process enhancement, together with significant CNO overabundances (Gonzalez and Wallerstein, 1994). ROA 24, V 1 and V29, with model parameters respectively (T_{eff} = 6250, log(g) = 1.0), (5250,1.0) and (5250,1.0) are somewhat cooler than our stars. They display a large Fe deficiency of [Fe/H] $\approx$ -2.0. Comparing the CNO abundances found for these three UV-bright stars with those of other UV-bright objects in the cluster, Gonzalez and Wallerstein (1994) found that the enhancements occur for $\log(L/L_{\odot}) >$

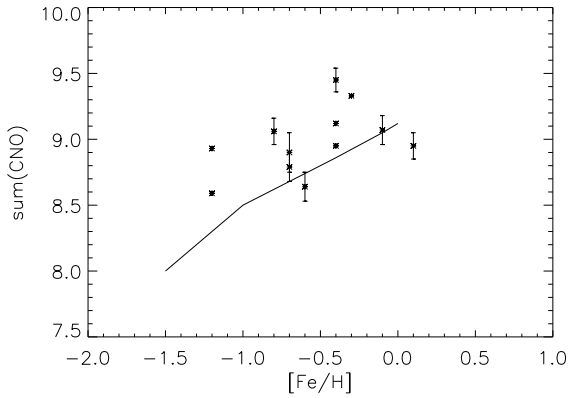

Fig. 9. The observed $\sum$ CNO abundance in function of the metallicity for the programme stars and other high-latitude F-supergiants in the literature.

Table 12. The measured total CNO abundance ($\sum$ CNO) compared to the expected value if only CNO-cycle material would have been mixed to the surface (labelled as $prim$). The difference of the two values is given in the last column.

Star	[Fe/H]	$\sum$ CNO	$\sum$ CNO$_{prim}$	$\Delta\sum$ CNO
HD 95767	+0.1	8.95	9.12	-0.17
SAO 239853	−0.8	9.06	8.62	+0.44
HD 108015	−0.1	9.07	9.06	+0.01
HD 112374	−1.2	8.59	8.30	+0.29
HD 131356	−0.6	8.64	8.74	-0.10
HD 133656	−0.7	8.90	8.68	+0.22
HD 158616	−0.7	8.79	8.68	+0.03
HD 187885	−0.4	9.45	8.86	+0.59
HD 161796	−0.3	9.33	8.92	+0.41
HR 6144	−0.4	9.12	8.86	+0.26
89 Her	−0.4	8.95	8.86	+0.09
HD 56126	−1.2	8.93	8.30	+0.63

2.5. Note, however, that the s-process elements are only mildly enhanced in the three stars. Moreover, C is significantly less enhanced than O and even N against expectation for a third dredge-up. A possibility is that the C and O produced in the He-burning layer have passed through a H-burning shell before coming to the surface (Gonzalez and Wallerstein, 1994). This effect complicates the interpretation of the relative abundances of CNO; the best evidence for the presence of He-burning products on the surface of the three stars is the increase of the *total* amount of CNO, together with the s-process elemental enhancements.

The abundance ratios found for the other stars are less easy to interpret. Except for the abovementioned HD 95767 and HD 108015, the ratios point to the evolved nature of the objects but strong chemical evidence for a post-AGB nature of the objects, e.g. s-process enhancement, large C overabundances, are not found. We discuss the CNO ratios now in more detail.

High N abundances point to mixing of CNO-cycled material. In unevolved objects, the N abundance scales with the Fe abundance ([N/Fe] = 0.0 for the metallicity range +0.3 > [Fe/H] > -2, Wheeler et al., 1989), which is not the case for our programme stars. If only the CNO-cycled material is mixed to the stellar surface the total CNO abundance should remain the primordial value as the C, N and O nuclei only serve as catalysts in the reaction. For mixing of only CNO-cycle products, one thus expects the N overabundance to be compensated by a C and possibly an O-deficiency. This is, however, not observed for the majority of the objects : most show also C overabundances. In Fig. 9 we plotted the total CNO abundances versus the metallicity of our programme stars and the other high-galactic-latitude supergiant stars from the literature. The full line in the Fig. represents the expected primordial value. For the O versus Fe abundance relation we used [O/Fe] ≈ -0.5[Fe/H] for $-1.0<$[Fe/H]<0.0 and for lower metallicities a constant value of [O/Fe] = +0.5 (Wheeler et al., 1989). For the error bars in the sum we used the internal errors of the C, N and O analysis as main indicator. Where only a few lines were available, we adopted 0.2 dex for the error on the abundance. The computed N, O, and to a lesser extent C abundances are much less affected by model parameter uncertainties, but the metallicity is. The error in the metallicity is estimated to be 0.2-0.3 dex on average.

In Table 12 we listed for every star the difference between the measured total CNO abundance and the expected primordial value. For the objects from the literature, no errors are given. We omitted SAO 173329 and HD 107369, as we have no quantitative results information on the O respectively C abundances of these stars.

The strongest evidence for the third dredge-up from the CNO abundances are found for HD 187785 and HD 56126. HD 158616 displays an anomalously low O abundance, so that for this star a total CNO abundance equal to the primordial value is found, despite the s-process enhancement.

Several other stars seem to have increased their total CNO abundance, be it only by a small amount. All stars, except HD 131356, lie above the curve of the expected primordial value (Fig. 9). For HD 112374, HD 133656, 89 Her and HR 6144 the difference is hardly significant. For HD 161796 and SAO 239853, on the other hand, the evidence for a third dredge-up from the total CNO is more pronounced. In these two stars, however, the C/O ratio is not significantly enhanced and the s-process elements follow the Fe deficiency or are even slightly more deficient. The high N-abundance and large total CNO abundance indicate that the stars are enriched in a mixture of hydrogen and He-burning products, but without measurable s-process enhancements.

It is interesting to note that the stars HD 187885, HD 56126 and SAO 239853, all three CNO enhanced, are very similar as far as their model parameters and the shape of the IR excess are concerned. The total masses of the circumstellar dust-shells as computed from the IR excess (Bogaert, 1994) are : M_d = 1.6 10^{-4} for HD 187885; M_d = 9.2 10^{-3} for HD 56126 and 1.0 10^{-3} for SAO 239853. But while the former two display high C/O ratios and s-process elemental enhancement, in the

latter the C/O ratio is small and there is evidence for a s-process deficiency instead (see Fig. 8 and 4). What the origin of the different chemical evolution of the three objects is, remains an open question.

A final remark concerns HD 107369, the star for which no IR excess is observed and the only object not showing Hα emission. The conservative upper limit indicates the star to be the only one in the sample to be C *deficient*. The expected sum of the C and N abundance for an unevolved Z = -1 metallicity star is 7.68, the measured sum is 7.63, in good accordance with mixing of the CN-cycle of the CNO hydrogen burning. Also O seems to be deficient : for an [Fe/H] of -1, one expects for unevolved objects an [O/Fe] = +0.5 (Wheeler et al., 1989), while we measured [O/Fe] = 0.0. Note that this discrepancy disappears for the lower gravity, cooler model ([O/Fe] = +0.5). For this model we get [N/Fe] = +0.9 and the upper limit for the C abundance is [C/Fe] = 0.0. A more accurate temperature and gravity estimate for this object would be welcome. Interestingly, the chemical patterns observed in HD 107369 resemble the ones of the high galactic latitude B stars identified as being in a post AGB evolutionary phase (Table 11). These metal poor B stars display strong C depletions and only modera te depletions of N and O relative to the solar value. For most of these stars, however, there is only an estimate of the upper limit of the Fe-abundance, which complicates the comparison with other objects (McCausland et al., 1992). In Table 11 we used the upper limit of the Fe-abundance as the true metal content. Note that for these objects, there is no purely chemical indication that the third dredge-up was effective; the identification of these objects as "post"-AGB comes from the low metal content, the locus in the HR-diagram and the detection of a nebula around two of the objects : LS IV -12°111 which has also an IR excess detected by IRAS (McCausland et al., 1992) and also BD+33°2642 (Napiwotzki et al., 1994) which is classified as one of the 11 known halo PN and displays very similar chemical characteristics as the B-type post-AGB objects. If the third dredge-up indeed took place in these objects, one has to invoke scenarios where the C abundance remains low (McCausland et al., 1992). Our chemical analysis does not support the common origin of the optically bright F-type post-AGB stars and the post-AGB B stars in the halo, except for HD 107369. Also kinematically the two groups of objects show different characteristics with the former group showing mere thick-disc kinematics (see Table 1) while the latter display genuine halo kinematics.

8. Concluding remarks

In this paper we discussed the chemical composition of a sample of post-AGB candidate stars. We could prove that the majority of the objects indeed belong to an old population : they are Fe-deficient and show the CNO abundance ratios typical for evolved low-mass stars. Exceptions are HD 95767 and HD 108015 for which we found a solar chemical content.

For only three objects (HD 187885, HD 158616 and HD 56126) is there conclusive *chemical* evidence that they occur in a post-AGB (i.e. post third dredge-up) evolutionary phase : high total CNO abundance, high C/O ratio, for the former star a suprasolar He content and–above all–a large overabundance of s-process elements for all three objects. To our knowledge these are the only high galactic latitude supergiants in the field to display these chemical characteristics. The chemical analysis of these three stars thus confirms the predictions of current ideas about the late stages of evolution of low-mass stars. On the other hand, it is perplexing that most objects are not conform to theoretical expectation.

The other programme stars, and other well studied high-galactic latitude F-supergiants, display no s-process enhancement and even depletion in some cases. The high N abundance and the mildly enhanced total CNO abundance indicate, however, that the atmospheres of these objects contain a mixture of CNO-cycled material and He-burning products. However, even the enhancement of the total CNO abundance is barely significant in several objects.

One object shows unique chemical characteristics : HD 107369. It is the only star in our sample displaying a C deficiency. The star has an abundance pattern very similar to the metal deficient, high-galactic B stars though to be in a post AGB evolutionary stage.

Acknowledgements. The author thanks Christoffel Waelkens and Rens Waters for the many instructive discussions. He also thanks the staff of the Geneva Observatory and the La Silla observatory. The referee Dr. V.V. Smith is also acknowledged for the careful reading of the manuscript. The author gratefully acknowledges support from the Belgian Fund for Collective Basic Research, under grants nr. 2.0048.90 and 2.0145.94. This research has made use of the SIMBAD database operated at CDS, Strasbourg, France.

References

Adams S., Seaton M.J., Howarth I.D., Aurice M., Walsh J.R., 1984, *MNRAS* 207, 471

Baschek B., Holweger H., Traving G., 1966, *Abhandl. Hamburger Sternwarte* VIII nr. 1

Bidelman W.P., 1951, *ApJ* 113, 304

Bogaert E., 1994, Ph. D. Thesis of K.U.Leuven

Boyarchuk A.A., Lyubimkov, L.S., Sakhibullin, N.A., 1985, Astrophysics 22, 203

Bond H.E, 1991, in IAU Symposium 145: "*Evolution of stars: the Photospheric Abundance connection*", eds. G. Michaud and A.V. Tutukov, Kluwer, Dordrecht, p. 341

Bond H.E., Philip A., 1973, *PASP* 85, 332

Bond H.E., Luck R.E., 1987, *ApJ* 312, 203

Brown J.A., Tomkin J., Lambert D.L., 1983, *ApJ* 265, L93

Bujarrabal V., Alcolea J., Planesas P., 1992, *A & A* 257, 701

Burger M., 1976, Ph. D. Thesis, Vrije Universiteit Brussel

Castelli F., 1988, *Puplications of the Astronomical Observatory Trieste* 1164

Clegg R.E.S., Peimbert M., Torres-Peimbert S., 1987, *MNRAS* 224, 761

Conlon E.S., McCausland R.J.H., Dufton P.L., Keenan F.P., 1993, in A. S. P. Conference Series Volume 45: "*Luminous High-Latitude stars*", ed: D.D. Sasselov, p. 146

Cramer N., Maeder A., 1979, *A & A* 78, 305

Delbouille L., Neven L., Roland G., 1973, Atlas photometrique du spectre solaire, Insitut d'Astrophysique, Université de Liège
Eggen O.J., 1986, *AJ* 91, 890
Eggen O.J., 1991, *AJ* 102, 1826
Evans T.L., 1985, *MNRAS* 217, 493
Führ J.R., Martin G.A., Wieze W.L., 1988, *Journal of Physical and Chemical Reference Data*, Supplement No. 4, Volume 17
Giridhar, S., Rao, N.K., Lambert, D.L., 1994, *ApJ* 437, 476
Gonzalez G., Wallerstein G., 1994, *AJ* 108, 1325
Gonzalez G., Wallerstein G., 1996, *MNRAS* 280, 515
Gonzalez G., Lambert D.L., Giridhar S., 1996, *ApJ* , in press
Grayzeck E.J., 1978, *AJ* 83, 1397
Grevesse N., 1989, in AIP Conference Series 183 : "*Cosmic Abundances of Matter*", ed. C.J. Waddington, Amarican Institute of Physics, New York, p.9
Hrivnak B.J., Kwok S., Volk K.M., 1989, *ApJ* 346, 265
Iben I. Jr., Renzini A., 1983, *Ann. Rev. Astron. Astrophys.* **21**, 271
Klochkova V.G., 1995, *MNRAS* 272, 710
Kodaira K., Philip A.G.D., 1984, *ApJ* 278, 208
Kodaira K., Greenstein J.L, Oke, J.B., 1970, *ApJ* 159, 485
Kurucz R.L., 1979, *ApJ Suppl. Ser.* 40, 1
Kurucz R.L., 1995, internet : http://cfa-www.harvard.edu/ẽsmond/kurtstcf.html
Kurucz R.L., Peytremann E., 1975, SAO Special Report 362
Kwok S., 1986, in : "*Late Stages of Stellar Evolution*", eds. S. Kwok and S.R. Pottasch, Astrophysics and Space Science Library, Vol. 132, 321
Kwok S., Hrivnak B.J., Boreiko R.T., 1987, *ApJ* 312, 303
Lambert D.L., Roby A.W., Bell R.A., 1982, *ApJ* 254, 663
Likkel L., Omont A., Morris M., Forveille T., 1987, *A & A* 173, L11
Luck R.E., 1993, in A. S. P. Conference Series Volume 45: "*Luminous High-Latitude stars*", ed: D.D. Sasselov, p. 87
Luck R.E., Lambert D.L., 1985, *ApJ* 298, 782
Luck R.E., Bond H.E., 1989, *ApJ* 342, 476
Luck R.E., Lambert D.L., Bond H.E., 1983, *PASP* 95, 413
Luck R.E., Bond H.E., Lambert D.L., 1990, *ApJ* 357, 188
Manchado A., Pottasch S.R., Garcia-Lario P., Esteban C., Mampaso A., 1989, *A & A* 214, 139
Mathis J.S., Lamers H.J.G.L.M., 1992, *A & A* 259, L39
McCausland R.J.H., Conlon E.S., Dufton P.L., Keenan F.P., 1992, *ApJ* 394, 298
Moore C.E., Minnaert M.G.J., Houtgast J., *National Bureau of standards Monograph 61*
Mulder P, 1984, *internal report of the astronomical institute of the University of Utrecht*
Napiwotzki R., Heber U., Köppen, J., 1994, *A & A* 292, 239
Oudmaijer R.D. 1996, A&A306, 823
Oudmaijer R.D., , van der Veen W.E.C.J., Waters L.B.F.M. et al., 1992, *A & A Suppl. Ser.* 96, 625
Parthasarathy M., Pottasch S.R., 1986, *A & A* 154, L16
Parthasarathy M., Pottasch S.R., Wamsteker W., 1988, *A & A* 203, 117
Parthasarathy M., Garcia Lario P., Pottasch S.R., 1992, *A & A* 264, 159
Pel J.W., 1976, *A & A Suppl. Ser.* 24, 413
Philip A., 1972, *ApJ* 171, 51
Pottasch S.R., Parthasarathy M., 1988, *A & A* 192, 182
Slijkhuis S., 1992, Ph. D. Thesis, Universiteit van Amsterdam, Nederland
Thévenin F., 1989, *A & A Suppl. Ser.* 77, 137
Thévenin F., 1990, *A & A Suppl. Ser.* 82, 179
Trams N.R., Waters L.B.F.M., Waelkens C. et al., 1991, *A & A Suppl. Ser.* 87, 361
van der Veen W.E.C.J., Habing H.J., Geballe T.R., 1989, *A & A* 226, 108
van der Veen W.E.C.J., Trams N.R., Waters L.B.F.M., 1993, *A & A* 269, 231
van der Veen W.E.C.J., Waters L.B.F.M., Trams N.R., Matthews H.E., 1994, *A & A* 285, 551
Van Winckel H., Mathis J.S., Waelkens C. 1992, Nature 356, 500
Van Winckel H., Waelkens C., Waters L.B.F.M., 1995, *A & A* 293, L25
Van Winckel H., Waelkens C., Waters L.B.F.M., 1996, *A & A* 306, L37
Van Winckel H., Oudmaijer R.D., Trams N.R., 1996b, *A & A* 312, 553
Venn K.A., 1993, *ApJ* 414, 316
Venn K.A., 1995a, *ApJ* 449, 839
Venn K.A., 1995b, *ApJ Suppl. Ser.* 99, 659
Venn K.A., Lambert, D.A., 1990, *ApJ* 363, 234
Volk K.M., Kwok S., 1987, *ApJ* 315, 654
Volk K.M., Kwok S., 1989, *ApJ* 342, 345
Waelkens C., Engelsman E., Waters L.B.F.M., van der Veen, W.E.C.J., 1989, in: "*From Miras to Planetary Nebulae: Which Path for Stellar Evolution ?*", eds. M.O. Mennessier, A. Omont, Edition Frontières, p. 470
Waters L.B.F.M., Trams N.R., Waelkens C., 1992, *A & A* 262, L37
Waters L.B.F.M., Waelkens C., Trams N.R., 1993, in: "*Mass loss on the AGB and Beyond*", ed H.E. Schwarz, 298
Wheeler J.C., Sneden C., Truran J.W. Jr., 1989, *Ann. Rev. Astron. Astrophys.* **27**, 279
Wiese W.L., Smith M.W., Glennon B.M., 1966, *NSRDS-NBS*, Vol I, 4

This article was processed by the author using Springer-Verlag LaTeX A&A style file *L-AA* version 3.